

Low-temperature behavior of single-domain through multidomain magnetite

Susan L. Halgedahl, Richard D. Jarrard

Department of Geology and Geophysics, University of Utah, Salt Lake City, UT 84112, USA

Received 19 October 1994; accepted after revision 10 December 1994

Abstract

We have investigated the low-temperature behavior of a suite of 'grown' synthetic and natural magnetites that span single-domain (SD) and multidomain (MD) behavior. Synthetic samples had been grown in the laboratory either in an aqueous medium or in glass. Natural samples included SD magnetites occurring in plagioclase and truly MD magnetites in the form of large octahedra. In all experiments a sample was first given a saturation remanence at room temperature; next, moment was measured continuously during cooling and warming between 230 K and 60 K. Similar to results reported earlier by other workers, magnetic memory is large in SD samples, whereas truly MD samples are almost completely demagnetized by cycling between room temperature and 60 K. Pseudo-single-domain samples exhibit behavior that is intermediate with respect to that of the SD and truly MD states. When data from this study are combined with data obtained by Hartstra [10] from sized, natural magnetites, it is found that the percentage of total remanence that survives cycling between room temperature and 60 K decreases linearly with the logarithm of grain size and, thus, with increasing number of domains. This relation suggests that memory can provide a reasonable estimate of grain size in those magnetite-bearing rocks for which these samples provide good analogues. Remarkably, some of the large natural octahedra provide a magnified view of MD response to low temperatures and thus reveal two surprising and intriguing types of behavior. First, below approximately 180 K these octahedra demagnetize through a series of large Barkhausen jumps. Second, near 117 K these same octahedra exhibit a 'wild zone', where magnetic moment executes large, random excursions. We interpret these two phenomena as direct evidence for the unpinning and irreversible displacement of domain walls in response to the drop in coercivity and, possibly, the broadening of domain walls as temperatures drop toward the isotropic point. One implication of this behavior is that cooling to progressively lower temperatures could provide an effective method for stepwise removal of paleomagnetic components carried by MD grains, even without passage through the isotropic point of magnetite.

1. Introduction

The low-temperature behavior of magnetite has been a subject of interest for many decades. At the isotropic point occurring at about 130 K, the first magnetocrystalline anisotropy constant, K_1 , changes sign, being negative above the

isotropic point and positive below it [1,2]. At the Verwey transition, which occurs at about 110–120 K, magnetite changes from cubic to what is now thought to be a monoclinic structure [3–5]. As a result, pre-existing remanence can drop dramatically when a sample passes through these transition temperatures [6–13]. In multidomain parti-

cles, demagnetization could result from the broadening, unpinning and complete reorganization of domain walls when K_1 becomes very small in the temperature range near the isotropic point. What remains puzzling is the partial recovery of original remanence after multidomain magnetite has been cycled through the transitions. Kobayashi and Fuller [8] suggested that stress centers both pin and cause retention of certain domain walls across the isotropic point. Although this specific mechanism remains somewhat speculative, Hodych [14] has demonstrated experimentally that stress does exert strong control on coercive force at low temperatures.

Not only is the low-temperature behavior of magnetite fascinating in terms of its physics, it also contains practical information relevant to rock magnetism and paleomagnetism. For example, the response of remanence to low-temperature cycling has been used as a magnetite detector in rocks [15,16]. Second, there is good evidence that magnetic memory increases with decreasing grain size, although the particular relationship depends on the sample preparation method [10,12,13,17–19]. In principle, low-temperature memory could provide a size estimate of the magnetites contained in rocks, once suitable synthetic analogues are available. Finally, with the increasing availability of instruments that enable remanence measurements at low temperature, continuous low-temperature demagnetization could become a viable technique for isolating paleomagnetic components in rocks highly susceptible to chemical alteration during heating above room temperature.

We have performed a suite of experiments to investigate low-temperature behavior in synthetic and natural 'grown' magnetite particles, encompassing the single-domain (SD) and multidomain (MD) states. The goals of these experiments were twofold:

- (1) to characterize low-temperature behavior across a broad range of grain size and thus domain state, since these grown crystals may be representative of magnetites occurring in certain types of rocks;
- (2) to investigate the physical mechanism by which low-temperature demagnetization oc-

curs in magnetite particles containing domain walls.

2. Samples and experimental methods

We used the following natural and synthetic samples generously provided by our colleagues: (1) plagioclase crystals separated magnetically from the Lambertville diabase and which contain submicron grains of magnetite (courtesy of R. Hargraves); (2) large (e.g., 0.5 mm) individual octahedra of natural magnetite occurring in schist from Chester, Vermont (courtesy of Harvard Museum); (3) very large (> 2 mm) individual octahedra of natural magnetite occurring in talc from Windham, Vermont (courtesy of Harvard Museum); (4) virgin, submicron magnetite cubes grown in aqueous (Aq) solution (courtesy of D. Dunlop); (5) glass-ceramic (GC) magnetite (courtesy of H.-U. Worm and W. Williams).

With the exception of the large, single octahedra, each sample contained an assemblage of particles. Lambertville samples were made by randomly dispersing the plagioclase crystal separate in nonmagnetic cement. Five GC magnetite samples were investigated; average particle sizes in these samples were 0.1 μm , 0.2 μm , 1.5 μm , 7 μm and 100 μm [20]. In the two Aq samples, average particle sizes were 0.1 μm and 0.22 μm , respectively [21]. To reduce magnetic interactions, the Aq magnetites were dispersed in calcium fluoride and then compressed into cylindrical pellets. It is important to note that the Aq magnetites had not been previously reduced [13].

Results of various rock magnetic experiments indicate that the magnetites above span the full range of domain states. In the five GC samples, hysteresis experiments yield the following ratios of saturation remanence to saturation moment (M_{rs}/M_s): 0.5 (0.1 μm); 0.44 (0.2 μm); 0.14 (1.5 μm); 0.03 (7 μm); 0.02 (100 μm) [22]. Note that in Worm and Markert's study of hysteresis properties versus grain size in GC magnetite assemblages [20], M_{rs}/M_s peaks at approximately 0.5 when grains are about 0.05 to about 0.1 μm in size. In finer grained assemblages M_{rs}/M_s is less than 0.5, due to the effect of superparamag-

netism; in coarser grained assemblages M_{rs}/M_s is less than 0.5, due to contributions from particles with walls. Thus, the 0.1 and 0.2 μm GC magnetite assemblages largely occupy the SD state after saturation, the 1.5 μm magnetite assemblage is largely pseudo-single-domain (PSD), and the 100 μm magnetite assemblage is truly MD. In 0.1 μm cubes grown in aqueous solution $M_{rs}/M_s = 0.202$, and in the 0.22 μm cubes $M_{rs}/M_s = 0.112$ [21]; thus, the submicron, Aq samples fall in the PSD range. In the Lambertville plagioclase, Cisowski [23] found that acquisition and alternating-field demagnetization curves of M_{rs} , when normalized to their maximum intensities, intersected near 0.5. This 50% intersection point provides strong evidence that remanence in the Lambertville plagioclase is carried by SD particles, as suggested much earlier by Hargraves and Young [24].

Despite their similar sizes, the submicron Aq magnetites and submicron GC magnetites exhibit very different values of M_{rs}/M_s . These differences could indicate that GC samples contain high levels of internal stress [25]. In a subsequent section, this difference will be discussed further in the context of low-temperature behavior.

At room temperature each sample was given a saturation remanent magnetization along one axis through exposure to a 5 kOe field generated with a bench-top electromagnet. Remanence was measured in a one-axis, SCT cryogenic susceptometer throughout thermal cycles between 230 and 60 K, so that samples passed through both the isotropic point and the Verwey transition. Average cooling and heating rates were 1 K/min. Owing to the thermocouple's location with respect to the sample in the susceptometer, most samples exhibited some thermal lag with respect to the thermocouple reading, as revealed by comparison of cooling to heating curves. In the majority of experiments, the working field inside the susceptometer was the ambient laboratory field ($\cong 0.4$ Oe). Samples were oriented with their remanences co-linear with the vertical axis read by the susceptometer. Unless otherwise noted, initial remanences pointed vertically downward during measurement. In a limited number of experiments a 10 Oe field was trapped in the susceptometer, so

that the effect of a moderate field on low-temperature behavior could be observed.

3. Results

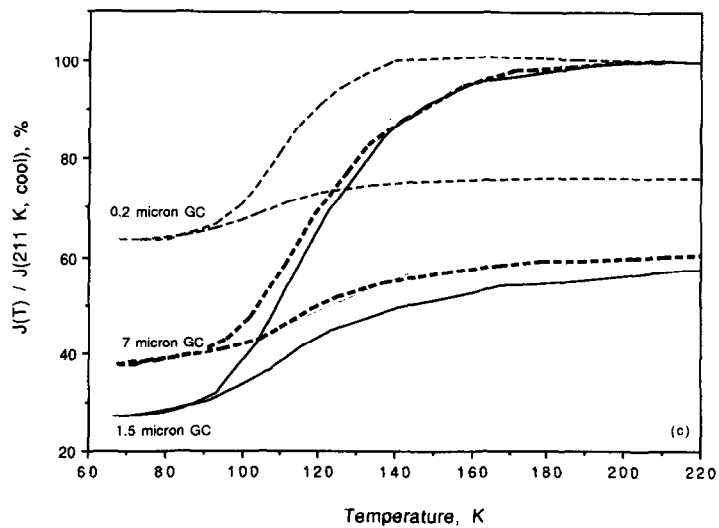
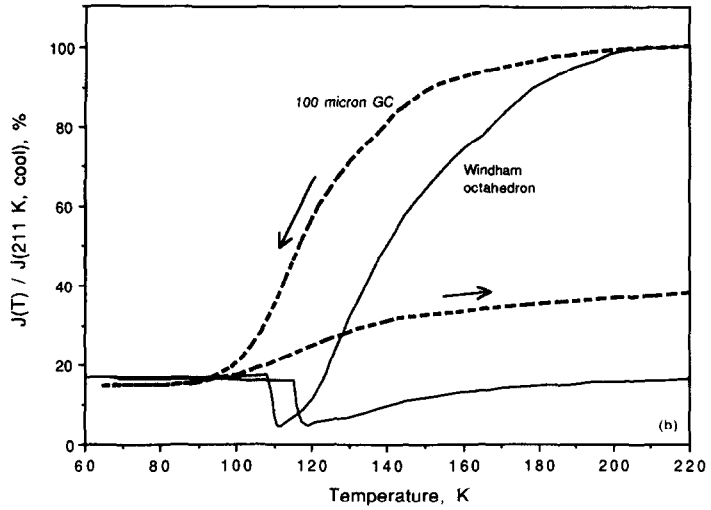
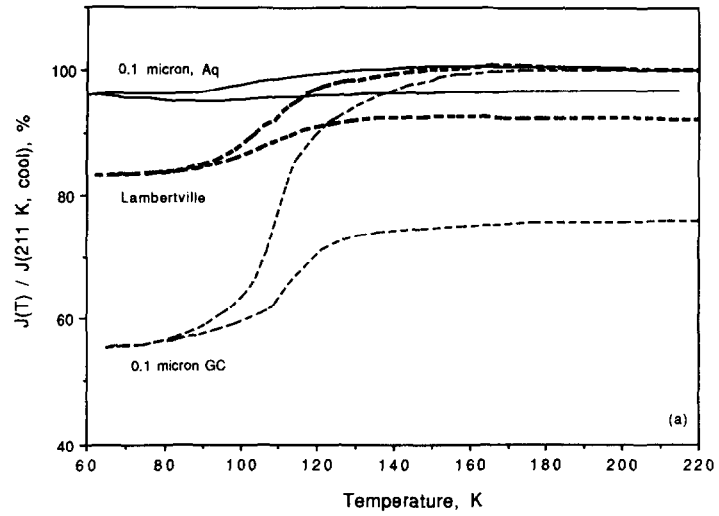
3.1. Low-temperature response curves and domain state

Typical cooling and heating curves for SD through truly MD magnetite assemblages are shown in Fig. 1. SD through PSD-type response is represented by the Lambertville plagioclase extract, the submicron GC magnetites and the submicron Aq magnetites (Fig. 1a and c). Truly MD behavior is represented well by 100 μm GC magnetite and by single magnetite octahedra from Windham, Vermont (Fig. 1b). As earlier authors have reported [9], SD and near-SD samples have large magnetic memories. Surprisingly, the 0.1 and 0.2 μm GC magnetites exhibit less memory than do the Aq magnetites, despite the GC samples having values of M_{rs}/M_s close to the ideal value of 0.5 for randomly oriented, uniaxial SDs (Fig. 1a and c); this result will be discussed shortly. As expected, truly MD samples exhibit a pronounced drop in remanence during cooling as the transition are approached, with little recovery during warming (Fig. 1b). GC magnetites in the 1–10 μm range display behavior that is intermediate between that of SD and truly MD particles (Fig. 1c).

Note that the large Windham octahedron displays a well defined minimum in its magnetic moment in the transition temperature range; below this range there is some recovery of moment (Fig. 1b). Hartstra [10] observed similar behavior in sized magnetite assemblages obtained by crushing rocks. However, the assemblages of smaller, dispersed particles studied here show no such minima.

3.2. Large Barkhausen jumps in large single crystals

Large octahedra of natural magnetite from Chester, Vermont, display two types of unexpected and intriguing behavior during thermal



cycles (Fig. 2a). First, below about 180 K the low-temperature response curve is punctuated by many sudden jumps in magnetic moment. Although most jumps are in the sense of decreasing moment, small positive jumps are not uncommon. Jumps are especially prominent when a field is applied opposite to the original remanence during a thermal cycle. Results of one such experiment are shown in Fig. 2b and c. In this example, a 10 Oe field was applied antiparallel to the saturation remanence during cooling and heating, resulting in jumps as large as 10^{-6} – 10^{-5} emu. Owing to the negative applied field, the moment reverses in the transition temperature range and, upon heating, the moment remains reversed. Qualitatively similar results are obtained in the earth's field, although the jumps are smaller in size. No jumps are observed at temperatures below the two transitions, but jumps appear again upon heating the crystal above the transitions.

The second surprising type of behavior is the presence of a 'wild zone' near the transitions, where the moment executes large, random excursions (Fig. 2a and b). Below the transitions no such excursions are observed. The wild zone also occurs during warming through the transitions, although the excursions are subdued with respect to those observed during cooling.

Note that the wild zone occurs in a somewhat lower interval of temperature during cooling than during warming (Fig. 2a). This difference most likely reflects thermal lag of the sample with respect to the thermocouple.

In the Chester crystal, Barkhausen jumps were first discovered between approximately 180 K and 120 K as rare drops in moment that were very much smaller than the initial remanence. This discovery was made when the instrument settings permitted an entire low-temperature run to be

displayed continuously on a recorder, without adjustments for the large drop of intensity between room temperature and the transitions. In order to resolve these jumps more clearly in subsequent experiments, the chart recorder signal was offset to zero and its gain was then increased several fold with respect to the setting used normally. Neither the Barkhausen jumps nor the wild zone was due to instrument noise, as indicated by the following four observations. First, the signal was smooth and displayed no discontinuities below the wild zone. Second, no jumps in the signal were observed when the crystal was held at a constant temperature in the range where large jumps ordinarily occurred during cooling or heating. Third, neither jumps nor a wild zone was detected in the assemblages, even when their low-temperature responses were viewed at an expanded scale. Fourth, not only were jumps observed in the Chester crystals during the several runs performed throughout the course of these experiments, but they were also observed on the same days when other samples, such as the assemblages, exhibited smooth low-temperature curves.

It is unknown whether the single Windham octahedra also exhibit large jumps. Because the Windham crystals were very large (e.g., several millimeters) and their moments very strong, the instrument gain could not be offset sufficiently to allow detection of possible jumps.

4. Physical mechanisms of low-temperature behavior

4.1. SD through PSD behavior

The Lambertville plagioclase extracts exemplify what has often been considered to be 'typi-

Fig. 1. (a) Response of room-temperature saturation remanence to low-temperature cycling in three samples of SD and PSD magnetite. $J(T)/J(211 \text{ K, cool})$ is the ratio of remanence measured at temperature T to the initial remanence at 211 K before cycling, in percent. Solid curve = $0.1 \mu\text{m}$ magnetite cubes grown in an aqueous (Aq) medium, without being reduced; bold dashed curve = submicron magnetite in plagioclase crystals extracted magnetically from the Lambertville diabase; dashed curve = $0.1 \mu\text{m}$ glass-ceramic (GC) magnetite. (b) Low-temperature response of saturation remanence carried by MD magnetite. Dashed curve = $100 \mu\text{m}$ GC magnetite; solid curve = $3 \mu\text{m}$ octahedron of natural magnetite from Windham, Vermont. (c) Low-temperature response of saturation remanence carried by three GC samples. Dashed curve = $0.2 \mu\text{m}$ GC magnetite; solid curve = $1.5 \mu\text{m}$ GC magnetite; bold dashed curve = $7 \mu\text{m}$ GC magnetite.

cal' SD response [9]. These samples exhibit a nearly 20% drop in remanence during cooling below about 120 K, but they recover more than 90% of their original remanence during warming to room temperature.

This observed behavior is very different from what one expects from SD crystals of pure magnetite lacking significant internal stress or shape anisotropy. In such an ideal assemblage memory should be low, for the following reasons: In the saturation remanent state, each particle's magnetization vector will point along the direction of form $\langle 111 \rangle$, which is closest to the direction of the previously applied field. Upon cooling through the isotropic point, the easy magnetocrystalline direction changes from $\langle 111 \rangle$, a body diagonal, to $\langle 100 \rangle$, a cube edge. At the Verwey transition, one of the cube edge directions becomes both the monoclinic c axis and the easy magnetocrystalline

axis in each crystal [2–5]. In zero field and, presumably, in a weak field, these c axes should be distributed with equal probability among the cube edge directions of all particles. During warming these transitions are reversed. Consequently, cooling through the isotropic point causes a particle's moment to flip from its original $\langle 111 \rangle$ direction to one of the nearest cube edges. Cooling through the Verwey transition may cause the particle's moment to flip from one cube edge direction to another, depending on which becomes the monoclinic c axis. Upon warming through the isotropic point, the moment will flip from a cube edge to the nearest direction along a body diagonal ($\langle 111 \rangle$); in general, this final direction will not coincide with that occupied in the original saturation remanent state. Thus, thermal cycling through the two transitions makes all of the $\langle 111 \rangle$ -type directions available to the magne-

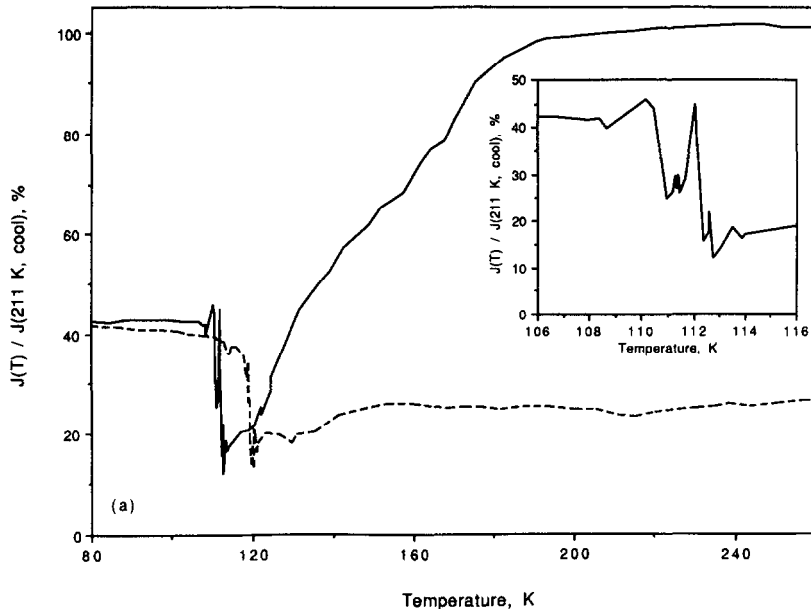


Fig. 2. Large Barkhausen jumps and 'wild zone' exhibited by a large natural octahedron of magnetite from Chester, Vermont, during a thermal cycle between 260 K and 70 K. (a) Complete low-temperature response curve of room-temperature saturation remanence carried by the Chester octahedron. Solid curve = cooling; dashed curve = heating. Note the presence of a 'wild zone' near 110 K on the cooling curve, where the moment undergoes large, random excursions. Inset: magnified view of the wild zone during cooling. (b) Moment of the Chester octahedron as a function of temperature during cooling in an external field of -10 Oe, starting from a state of saturation remanence with positive polarity. Segments of the low-temperature response curve are offset vertically, in order to display the many Barkhausen jumps observed during cooling. Note that the moment reverses at about 120 K. The wild zone can be seen at about 112 K. (c) Amplified view showing large Barkhausen jumps along a segment of the Chester octahedron's cooling curve.

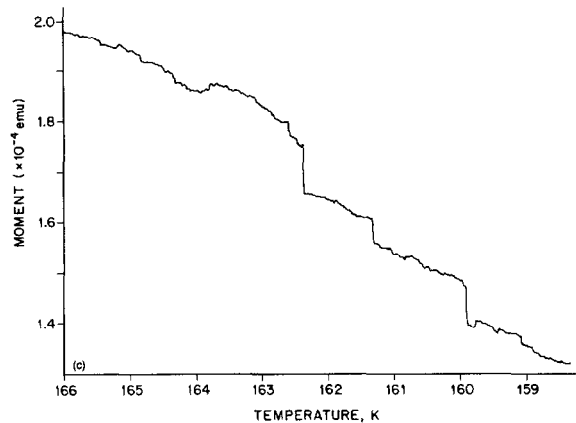
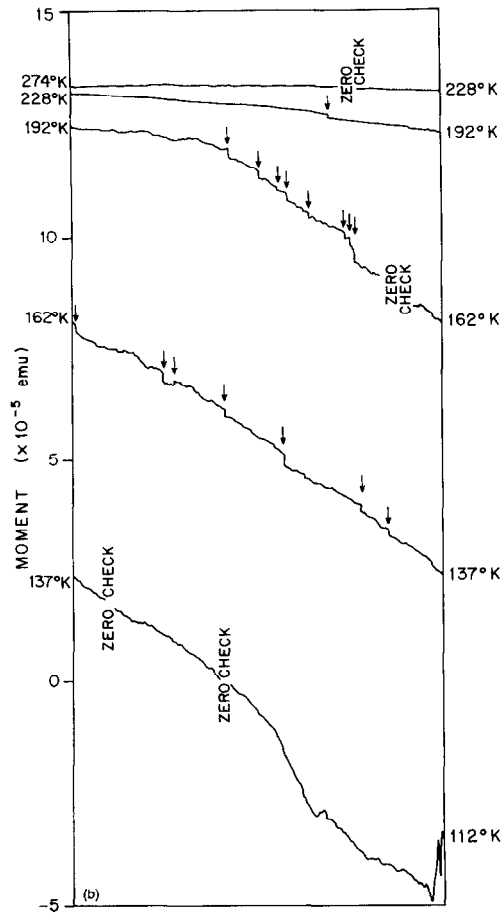


Fig. 2 (continued).

tization vectors. As a result, there survives only a small net component parallel to the population's original saturation remanence, and memory is low (e.g., see discussion in [18]).

Clearly, the Lambertville magnetites do not conform to the behavior predicted above. Yet the observed drop in remanence during cooling indicates that cubic magnetocrystalline energy cannot be dismissed. A simple explanation for the behavior observed here is that the majority of Lambertville magnetites are controlled by stress or shape anisotropy, while magnetocrystalline anisotropy dominates the small remainder of the population.

However, the behavior of Lambertville magnetites must also be considered in the context of

recent work by Özdemir et al. [13], who demonstrated that the low-temperature response of sub-micron magnetite is strongly sensitive to room temperature oxidation. They discovered that the Verwey transition and isotropic point are partly or almost completely suppressed in dispersions of virgin, aqueously grown, submicron magnetite cubes (0.037, 0.076, 0.1 and 0.22 μm in diameter). Also, the degree of suppression increases as grain size goes down. This suppression is interpreted as indicating surface oxidation to maghemite, in which the two transitions are absent, because, after reduction in a CO-CO_2 atmosphere, the transitions are pronounced in these same dispersions [13].

The high memory and low-temperature curves

of the Lambertville magnetite, therefore, are not inconsistent with partial oxidation of magnetite to maghemite. However, we view this explanation with caution for two reasons. First, the fine magnetites have probably been shielded from oxidation by their plagioclase hosts. Second, thermal demagnetization curves of weak-field thermoremanent magnetization are flat, until unblocking occurs between 550° and 575°C [24]. Thus, thermomagnetic analyses show no evidence of magnetic minerals other than magnetite. Nevertheless, future work is needed to determine whether these magnetites are cloaked by an oxidized layer.

Low-temperature behavior of the synthetic, submicron magnetite samples appears to contradict the behavior ordinarily expected from their room-temperature hysteresis properties and implied domain states. In the two submicron GC samples, M_{rs}/M_s is near or equal to 0.5, the ideal value for a random assemblage of uniaxial SD grains. In contrast, the two submicron assemblages of Aq magnetite yield M_{rs}/M_s values typical of the PSD state. Yet the 0.1 μm Aq magnetites exhibit higher memory than do the GC samples of similar grain size. Furthermore, the drop in remanence at low temperatures is much smaller in the submicron Aq samples than in the submicron GC samples (Fig. 1a).

These differences may be partly explained by the results of Özdemir et al. [13]. In the present study, the Aq submicron magnetite came from the original batches used by Özdemir et al. [13], without being reduced. As shown in Fig. 1a, the cooling and warming curves of the 0.1 μm Aq particles show very little structure. This result agrees well with Özdemir et al.'s [13] results obtained by warming unreduced, companion samples from 5 K through the transitions. Apparently, virgin, Aq submicron magnetite cubes consist of a pure magnetite core, a mantle of maghemite, and an intervening transition zone of partial oxidation [13]. In small, partially oxidized magnetite particles that contain walls, a substantial percentage of the walls' surface areas would occupy the transition zone and, thus, low-temperature response would be subdued.

Unlike fine magnetites grown in water, the submicron GC magnetites grew in a silicate ma-

trix. It is probable that this matrix protected the magnetite crystals from surface oxidation; therefore, one would not expect oxidation to suppress the transitions in these samples. Nevertheless, one does expect a subdued low-temperature response, because $M_{rs}/M_s \cong 0.5$, the value indicative of SD grains dominated by uniaxial anisotropy, not cubic magnetocrystalline anisotropy. Clearly, this expectation is not fulfilled (Fig. 1a and c).

We suggest that the nucleation of walls at low temperature could contribute substantially to the sharp drop in moment that submicron GC magnetites exhibit near the transitions. Domain theory predicts that 0.1–0.2 μm magnetite particles should contain domain walls at room temperature, if the particles occupy an absolute minimum energy state and are stress free [26–29]. Yet, at room temperature, GC magnetite assemblages in this size range appear to be largely SD after exposure to a strong field. Two effects could produce this SD state. First, high internal microstress could raise the SD boundary size at room temperature, with respect to that usually predicted for stress-free grains. High levels of microstress in these samples would not be surprising, because synthesis involved quenching from high temperature [20]. Indeed, above 293 K the temperature dependence of coercive force in GC samples supports stress control [25]. Second, when combined with magnetocrystalline anisotropy, internal stress would raise the internal nucleation field, $2K_{\text{tot}}/J_s$ (where K_{tot} = total anisotropy energy and J_s = spontaneous magnetization), required to form walls at room temperature. This could inhibit nucleation of walls in the saturation remanent state, even though walls are energetically favorable [2,30,31]. As the isotropic point is approached during cooling, the large drop in K_1 and the smaller drop in the magnetostriction constant, λ_{111} , would lower both the domain wall energy and the nucleation field. Also, the equilibrium number of domains would increase. The net result would be the increasing accessibility of equilibrium domain states and the addition of energetically favorable walls in some grains. Indeed, Boyd et al. [32] have reported that low-temperature cycling does trigger the nucle-

ation of walls in large magnetite particles that initially appear to be saturated at room temperature. Consequently, the sharp transition exhibited by 0.1 and 0.2 μm GC magnetites could reflect nucleations in grains that were metastable SDs after saturation at room temperature. This hypothetical mechanism requires further experimental testing.

4.2. Truly MD behavior

In contrast to SD grains, low-temperature demagnetization in truly MD particles is largely irreversible and magnetic memory is low. Remarkably, octahedra from Chester, Vermont, provide a magnified view of this process. As indicated by curves shown in Fig. 2, between about 180 and 120 K demagnetization occurs mainly through many Barkhausen jumps, some of which are quite large. In this temperature range these jumps are not attributable to thermal activation of walls over low barriers, since jumps were not observed when temperature was held constant. The probable mechanism for these jumps is the unpinning of domain walls as the sample cools below about 180 K, as would result from a large drop in coercivity as K_1 and λ_{111} decrease below this temperature [2,14,33]. This mechanism is supported by the observation that increasing the intensity of a field directed antiparallel to remanence causes the jumps to increase in magnitude. This response is expected from a wall-unpinning mechanism, since a back-field would reinforce a particle's demagnetizing field. One predicted consequence of this mechanism is that substantial demagnetization could be accomplished in zero field simply by cooling a MD sample from room temperature to temperatures in the range of 180–130 K, without passage through the isotropic point.

The existence of a 'wild zone' strongly suggests that walls become highly unstable in the temperature range encompassing one or both of the transitions. Such instability could be rooted in four phenomena: (1) the substantial broadening of walls when K_1 is small; (2) low microcoercivities, owing to the low magnitudes of K_1 and, to a lesser extent, of λ_{111} ; (3) increased number of

domains, in response to the low magnitude of K_1 ; and (4) reorientation of M_s . In order to pin walls effectively, a defect must have a 'zone of pinning' at least comparable to wall width. Thus, defects would have little or no pinning power if walls grew very much broader than the defects themselves. As a result, random fluctuations of small stray fields could drive walls through large, random excursions at temperatures where K_1 is low. Even in the absence of stray fields, thermal activation could trigger large, random jumps if barriers were virtually 'invisible' to very broad walls. Finally, wall nucleation and dramatic reorganization of the domain structure could result from: (1) the ultralow magnitude of K_1 and, thus, of wall energy near the isotropic point [31,34]; and (2) changes in easy axes at both the isotropic point and at the Verwey transition [11,12].

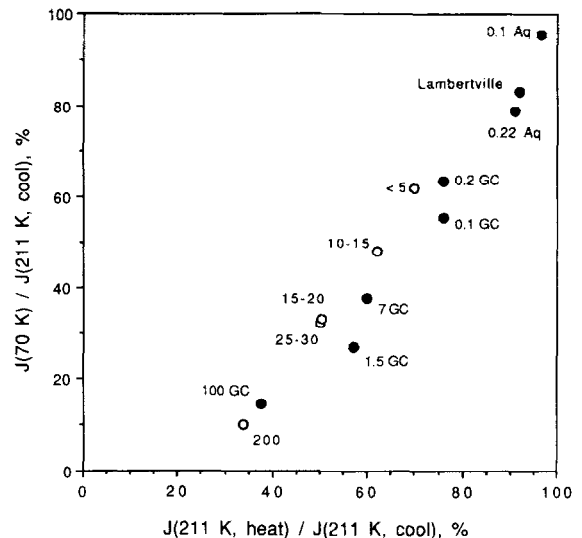


Fig. 3. Plot of memory ratios $J(70 \text{ K})/J(211 \text{ K, cool})$ against $J(211 \text{ K, heat})/J(211 \text{ K, cool})$ for magnetites of different provenances and grain sizes. $J(211 \text{ K, cool})$ is saturation remanence measured at 211 K during cooling; $J(70 \text{ K})$ is remanence measured at 70 K; $J(211 \text{ K, heat})$ is remanence measured at 211 K during warming. Ratios are expressed in percent. ● = grown magnetite crystals initially carrying saturation remanence, this paper, GC = glass-ceramic samples, Aq = magnetite cubes grown in an aqueous medium; Lambertville = magnetite-bearing plagioclase needles extracted from the Lambertville diabase; ○ = crushed natural magnetite initially carrying saturation remanence, from Hartstra [10]. Numbers specify grain size in microns.

5. Future applications to paleomagnetism and rock magnetism

Similar to Hartstra [10], we have defined two low-temperature memory ratios:

$$J(70 \text{ K})/J(211 \text{ K, cool})$$

and:

$$J(211 \text{ K, heat})/J(211 \text{ K, cool})$$

where $J(211 \text{ K, cool})$ is saturation remanence measured at 211 K during cooling, $J(70 \text{ K})$ is remanence measured at 70 K, and $J(211 \text{ K, heat})$ is remanence measured at 211 K during warming. $J(70 \text{ K})/J(211 \text{ K, cool})$ represents the degree to which a sample demagnetizes during cooling through the transitions, while $J(211 \text{ K, heat})/J(211 \text{ K, cool})$ represents the degree to which remanence rebounds after a thermal cycle. In the present samples, $J(211 \text{ K, cool})$ and $J(211 \text{ K, heat})$ are virtually equal to the remanences measured at 293 K during cooling and heating, respectively.

The two memory ratios of grown magnetite crystals studied here and of the natural, crushed magnetite particles studied by Hartstra [10] are plotted in Fig. 3. Despite their very different provenances, these two suites of samples define very similar trends. Both the percentage of remanence that survives below the transitions and percentage of total rebound during warming increase systematically with decreasing grain size and, thus, with decreasing number of domains.

As Fig. 3 suggests, low-temperature remanence parameters could provide a means of estimating particle size. Such a grain size indicator would be especially useful in the case of rocks containing magnetites which were either below the limit of optical resolution or of very low abundance. By far the most experimentally accessible memory parameter is $J(211 \text{ K, heat})/J(211 \text{ K, cool})$, the percentage of saturation remanence that survives low-temperature cycling. Because this ratio changes very little between 211 K and room temperature, it can be obtained readily by

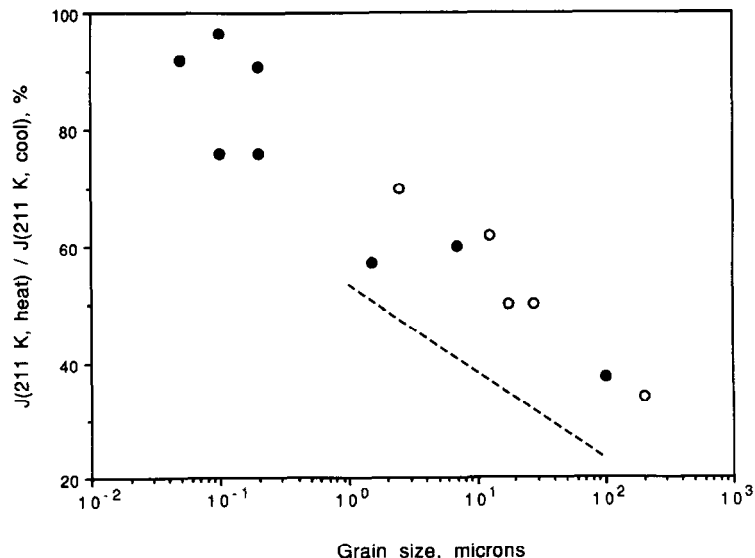


Fig. 4. Semilogarithmic plot of the memory ratio $J(211 \text{ K, heat})/J(211 \text{ K, cool})$, in percent, against grain size for the magnetite samples studied here and samples studied by Hartstra [10]. $J(211 \text{ K, cool})$ is saturation remanence measured at 211 K before a complete low-temperature cycle; $J(211 \text{ K, heat})$ is remanence measured at 211 K after a low-temperature cycle. Note that $J(211 \text{ K, cool})$ and $J(211 \text{ K, heat})$ are virtually identical to remanences measured at room temperature before and after thermal cycling, respectively. ● = grown magnetite particles initially carrying saturation remanence, this paper (see Fig. 3); ○ = crushed natural magnetite initially carrying saturation remanence, from Hartstra [10]; dashed line = regression line from crushed, sized magnetite studied by Parry [17,18].

first measuring saturation remanence at room temperature, immersing the sample in liquid nitrogen, and then measuring remanence after the sample has been allowed to warm.

In Fig. 4, $J(211 \text{ K, heat})/J(211 \text{ K, cool})$ is plotted against average grain size, d , for the samples studied here and the samples studied by Hartstra [10]. For these particular data, linear regression yields $J(211 \text{ K, heat})/J(211 \text{ K, cool}) = 0.714 - 0.068 \ln(d)$, where d is in microns (correlation coefficient = 0.88).

Without geologic constraints, however, one cannot yet apply a 'magic bullet' approach to deduce the grain size of magnetite from low-temperature memory or from the shape of low-temperature curves. Heider et al. [12] have compiled memory ratios for a variety of magnetite samples, including hydrothermally grown crystals, crushed powders, aqueously grown magnetite cubes after reduction, powders produced by reducing hematite pigments, two GC samples and several large single crystals. These many results reveal no single relationship between memory and grain size for all samples. Instead, the grain-size dependence of memory reflects the sample synthesis method.

Nevertheless, the compilation of Heider et al. [12] reveals four clear differences between free-grown magnetites (magnetite crystals synthesized without a matrix, such as hydrothermally grown crystals, aqueously grown crystals and magnetite grown by reducing hematite) and crushed magnetites:

- (1) M_{rs} memories of free-grown magnetites drop much more rapidly with increasing grain size than do memories of crushed magnetites;
- (2) when free-grown magnetites are larger than about $10 \mu\text{m}$, their M_{rs} memories are low (e.g. ≤ 0.25) and are not dependent on grain size;
- (3) crushed magnetites between about 1 and $200 \mu\text{m}$ in size show a systematic decrease in M_{rs} memory with increasing grain size;
- (4) for any given grain size in the range of about $1\text{--}100 \mu\text{m}$, free-grown magnetites exhibit far less memory than do magnetites obtained by crushing. At sizes above about $100 \mu\text{m}$ the two species of samples exhibit low memories

of similar magnitude (e.g., ≤ 0.20). This latter similarity could result from the truly MD behavior of both sample species when grain size is very large.

These four differences undoubtedly reflect the very different levels of internal microstress in the two sample classes: internal microstress is quite low in free-grown crystals but high in crushed grains.

To date, do any of the synthetic or crushed magnetites studied at low temperatures represent natural magnetites in rocks? In our view, the answer is yes with respect to a few types of synthetic samples and a few rock types. Although probably too highly stressed to represent magnetites in very young, poorly compacted sedimentary rock or in slowly cooled igneous rock, crushed and GC magnetites could share similar stress states with magnetites in rapidly cooled subaerial lavas and in the chilled margins of dikes. In their unreduced state [13], submicron, Aq magnetite cubes could represent fine, diagenetic magnetites that have grown in soils and some sedimentary rocks and that have subsequently undergone some degree of in situ low-temperature oxidation to maghemite. Magnetite particles grown hydrothermally at elevated temperatures are more problematic. Owing to their high compositional purity, high degree of crystallinity, relatively low density of defects, and low state of internal microstress, hydrothermally grown magnetites may have few natural counterparts that are important to NRM. Nevertheless, hydrothermally grown magnetites are a critical member of the microstress spectrum and thus contribute to our understanding of how stress, or the lack of stress, affects remanence and stability.

Clearly, there are large gaps between the stress states of most synthetic magnetite samples and the natural magnetites found in the wide variety of rocks relevant to paleomagnetism. Thus, there are still unacceptably large uncertainties associated with using memory to estimate grain size in magnetite-bearing rocks. These uncertainties emphasize the need for two suites of reference samples for future low-temperature studies: (1) magnetite-bearing rocks of various petrogenetic origins, where each sample contains magnetite with

a narrow range of grain size; and (2) suitable synthetic analogues containing magnetites whose microstress levels represent natural states.

These experiments provide the first direct evidence that MD particles steadily demagnetize at low temperatures through a series of irreversible wall displacements. If future experiments demonstrate this interpretation to be correct, it follows that remanence rebound would be incomplete even when a MD sample is cooled to a temperature substantially above the range encompassing the isotropic point and the Verwey transition. This suggests an alternate method of stepwise demagnetization: a sample would be cooled to progressively lower temperatures between about 180 and 130 K, and after each cooling step the sample would be warmed to room temperature and then measured. After low-temperature demagnetization was complete, the surviving remanence would be demagnetized with conventional techniques. This method could remove MD components carried by rocks that were subject to chemical change during repeated heatings; in addition, it would allow the MD component to be resolved accurately on a vector end point diagram. Finally, it could provide an especially effective tool for removing MD, viscous components whose coercivity and/or unblocking temperature spectra overlapped with the spectra associated with PSD or SD grains carrying the characteristic component of natural remanence.

Acknowledgements

The authors wish to thank Bruce Moskowitz and David Dunlap for their helpful reviews. This work was funded by NSF grants EAR91-21015 and EAR92-04762. [RV]

References

- [1] L.R. Bickford, J.M. Brownlow and R.F. Penoyer, Magnetocrystalline anisotropy in cobalt-substituted magnetic single crystals, *Proc. Inst. Electr. Eng.* B104, 238–244, 1957.
- [2] Y. Syono, Magnetocrystalline anisotropy and magnetostriction of Fe_3O_4 – Fe_2TiO_4 series — with special application to rock magnetism, *Jpn. J. Geophys.* 4, 71–143, 1965.
- [3] E.J.W. Verwey and P.W. Haayman, Electronic conductivity and transition point in magnetite, *Physica* 8, 979, 1941.
- [4] N. Otsuka and H. Sato, Observation of the Verwey Transition in Fe_3O_4 by high-resolution electron microscopy, *J. Solid State Chem.* 61, 212–222, 1986.
- [5] J.M. Zuo, J.C.H. Spence and W. Petuskey, Charge ordering in magnetite at low temperatures, *Phys. Rev. B* 42, 8451–8464, 1990.
- [6] T. Nagata, K. Kobayashi and M.D. Fuller, Identification of magnetite and hematite in rocks by magnetic observation at low temperature, *J. Geophys. Res.* 69, 2111–2120, 1964.
- [7] M. Ozima, M. Ozima and S. Akimoto, Low temperature characteristics of remanent magnetization of magnetite, *J. Geomagn. Geoelectr. Jpn.* 16, 165–177, 1964.
- [8] K. Kobayashi and M. Fuller, Stable remanence and memory of multi-domain materials with special reference to magnetite, *Philos. Mag.* 18, 601–624, 1968.
- [9] S. Levi and R.T. Merrill, Properties of single-domain, pseudo-single-domain, and multidomain magnetite, *J. Geophys. Res.* 83, 309–323, 1978.
- [10] R.L. Hartstra, TRM, ARM and Isr of two natural magnetites of MD and PSD grain size, *Geophys. J. R. Astron. Soc.* 73, 719–737, 1983.
- [11] K.S. Argyle and D.J. Dunlop, Low-temperature and high temperature hysteresis of small multidomain magnetites (215–540 nm), *J. Geophys. Res.* 95, 7069–7083, 1990.
- [12] F. Heider, D.J. Dunlop and H.C. Soffel, Low-temperature and alternating field demagnetization of saturation remanence and thermoremanence in magnetite grains (0.037 mm to 5 mm), *J. Geophys. Res.* 97, 9371–9381, 1992.
- [13] O. Özdemir, D.J. Dunlop and B.M. Moskowitz, The effect of the Verwey transition in magnetite, *Geophys. Res. Lett.* 20, 1671–1674, 1993.
- [14] J.P. Hodych, Magnetostrictive control of coercive force in multidomain magnetite, *Nature* 298, 542–544, 1982.
- [15] M. Jackson, Diagenetic sources of stable remanence in remagnetized Paleozoic cratonic carbonates: A rock magnetic study, *J. Geophys. Res.* 95, 2753–2761, 1990.
- [16] M. Jackson, P. Rochette, G. Fillion, S. Banerjee and J. Marvin, Rock magnetism of remagnetized Paleozoic carbonates: low-temperature behavior and susceptibility characteristics, *J. Geophys. Res.* 98, 6217–6225, 1993.
- [17] L.G. Parry, Magnetization of multidomain particles of magnetite, *Phys. Earth Planet. Inter.* 19, 21–30, 1979.
- [18] L.G. Parry, Shape-related factors in the magnetization of immobilized magnetite particles, *Phys. Earth Planet. Inter.* 22, 144–154, 1980.
- [19] D.J. Dunlop and K.S. Argyle, Separating multidomain and single-domain-like remanences in pseudo-single-domain magnetites (215–540 nm) by low-temperature demagnetization, *J. Geophys. Res.* 96, 2007–2017, 1991.

- [20] H.-U. Worm and H. Markert, Magnetic hysteresis properties of fine particle titanomagnetites precipitated in a silicate matrix, *Phys. Earth Planet. Inter.* 46, 84–92, 1987.
- [21] D.J. Dunlop, Hysteresis properties of magnetite and their dependence on particle size: a test of pseudo-single-domain models, *J. Geophys. Res.* 91, 9569–9584, 1986.
- [22] W. Williams, The effect of time and temperature on magnetic remanence, Ph.D. Thesis, Cambridge Univ., 1986.
- [23] S. Cisowski, Interacting vs. non-interacting single domain behavior in natural and synthetic samples, *Phys. Earth Planet. Inter.* 26, 56–62, 1981.
- [24] R.B. Hargraves and W.M. Young, Source of stable remanent magnetism in Lambertville diabase, *Am. J. Sci.* 267, 1161–1177, 1969.
- [25] H.-U. Worm, M. Jackson, P. Kelso and S.K. Banerjee, Thermal demagnetization of partial thermoremanent magnetization, *J. Geophys. Res.* 93, 12,196–12,204, 1988.
- [26] R.F. Butler and S.K. Banerjee, Theoretical single-domain grain-size range in magnetite and titanomagnetite, *J. Geophys. Res.* 80, 4049–4058, 1975.
- [27] T. Moon and R.T. Merrill, The magnetic moments of non-uniformly magnetized grains, *Phys. Earth Planet. Inter.* 34, 186–194, 1984.
- [28] R.J. Enkin and D.J. Dunlop, A micromagnetic study of pseudo-single-domain remanence in magnetite, *J. Geophys. Res.* 92, 12,726–12,740, 1987.
- [29] W. Williams and D.J. Dunlop, Three-dimensional micromagnetic modelling of ferromagnetic domain structure, *Nature* 337, 634–637, 1989.
- [30] W.F. Brown, *Micromagnetics*, 143 pp., Wiley, New York, 1963.
- [31] S. Halgedahl and M. Fuller, The dependence of magnetic domain structure upon magnetization state with emphasis upon nucleation as a mechanism for pseudo-single-domain behavior, *J. Geophys. Res.* 88, 6505–6522, 1983.
- [32] J.R. Boyd, M. Fuller and S. Halgedahl, Domain wall nucleation as a controlling factor in the behaviour of fine magnetite particles in rocks, *Geophys. Res. Lett.* 11, 193–196, 1984.
- [33] J.P. Hodych, Low-temperature demagnetization of saturation remanence in rocks bearing multidomain magnetite, *Phys. Earth Planet. Inter.* 66, 144–152, 1991.
- [34] S. Halgedahl, Domain pattern observations in rock magnetism: progress and problems, *Phys. Earth Planet. Inter.* 96, 127–163, 1987.